HydrogeoEstimatorXL: an Excel-based tool for estimating hydraulic gradient magnitude and direction

J.F. Devlin[1] and P.C. Schillig[2]

[1]Dept. of Geology, University of Kansas, Lindley Hall rm 120, 1475 Jayhawk Blvd., Lawrence, KS, 66049. email: jfdevlin@ku.edu, Tel: 785-864-4994
2Geosyntec Consultants, 289 Great Road Suite 105, Acton, MA 01720; 978-206-5749; email: PSchillig@Geosyntec.com

Abstract

HydrogeoEstimatorXL is a free software tool for the interpretation of flow systems based on spatial hydrogeological field data from multi-well networks. It runs on the familiar Excel spreadsheet platform. The program accepts well location coordinates and hydraulic head data, and returns an analysis of the area flow system in twodimensions based on a) a single best fit plane of the potentiometric surface and b) three-point estimators, i.e., well triplets assumed to bound planar sections of the potentiometric surface. The software produces graphical outputs including histograms of hydraulic gradient magnitude and direction, groundwater velocity (based on a site average hydraulic properties), as well as mapped renditions of the estimator triangles and the velocity vectors associated with them. Within the software, a transect can be defined and the mass discharge of a groundwater contaminant crossing the transect can be estimated. This kind of analysis is helpful in gaining an overview of a site's hydrogeology, for problem definition, and as a review tool to check the reasonableness of other, independent calculations. . The software is free of charge and available at http://hdl.handle.net/1808/22049 .

1. Introduction

The most common method of estimating groundwater discharge, Q (L^3/T), specific discharge, q (L/T), velocity, v (L/T), or contaminant (advective) mass flux, J (M/L^2T) is based on Darcy's Law (eq 1),

$$Q = -KA\frac{\Delta H}{\Delta x} \quad\quad (1)$$

$$q = \frac{Q}{A} = -K\frac{\Delta H}{\Delta x} \quad\quad (2)$$

$$v = \frac{q}{n} = -\frac{K}{n}\frac{\Delta H}{\Delta x} \quad\quad (3)$$

$$J = Cq = -CK\frac{\Delta H}{\Delta x} \quad\quad (4)$$

where A is the area cross-sectional to flow (L^2), K is hydraulic conductivity (L/T), H is total hydraulic head ($H=z+\Psi$), z is elevation head (L), Ψ is pressure head (L), x is distance in the direction of flow (L), and C is contaminant

concentration (M/L^3). The terms L, M, T are generalized units referring to distance, mass, and time, respectively. Typically, site investigations concerned with groundwater flow begin with evaluations of K and the hydraulic gradient ($\Delta H/\Delta x$). The evaluation of K has received enormous attention over the years. It was a chief motivation for the development of field methods including pumping tests (Kruseman and DeRitter, 1991), slug tests (Butler, 1997), direct push-based techniques (Butler *et al.,* 2002; 2007), flow meters (Molz *et al*., 1989), and geophysical techniques including ground penetrating radar (Knight, 2001) and nuclear magnetic resonance (NMR) (Legchenko *et al.*, 2002). It was also connected to laboratory techniques including grain size analyses (summarized in Devlin, 2015) and permeametry (Freeze and Cherry, 1979). However, while K is essential to know for a complete description of a site's hydrogeology, including predictions of groundwater speed, it is not essential to know for mapping the general steady-state patterns of flow at a site, i.e., flow directions. Patterns of flow across an area depend on the variations in hydraulic gradient, and these develop with an inherent accounting for aquifer heterogeneity that does not depend on a specific knowledge of K, at least as a first approximation.

Misleading interpretations of groundwater velocity can result from errors that commonly occur in hydraulic head data sets, and are propagated through gradient estimations. Examples were described by Silliman and Frost (1998), Zemansky and Devlin (2014) and Schillig *et al.* (2016), and arise from a variety of causes (see section 'Example Case 1'). The purpose of this article is to introduce an Excel-based tool, *HydrogeoEstimatorXL*, for evaluating hydraulic gradients as either single plane surfaces or more complex surfaces characterized by three point estimators, i.e., well triplets each defining a separate planar surface. The calculations performed in *HydrogeoEstimatorXL* are well known and generally accepted for characterizing groundwater flow from field data. Therefore, the contribution here comes from the creation of a free tool that assembles the calculations into an easy-to-use package within a spreadsheet platform that is widely used and readily accessible to practitioners. Further, the graphical displays preset in *HydroGeoEstimatorXL* help users assess general trends in flow direction and magnitude and to identify the

presence of unrepresentative data points, providing hydrogeologists with a simple, preliminary means of examining water level data and maintaining quality assurance in hydrogeological datasets. The analysis can be completed by personnel without a lot of training in groundwater flow modeling, yet the results may be useful for model validation by highly trained modelers. The software is available free of charge at the University of Kansas Scholarworks site (http://hdl.handle.net/1808/22049) , and at the author's website:

http://www.people.ku.edu/~jfdevlin/Software.html

2. Background

A common method of determining the hydraulic gradient is to plot measured values of hydraulic head on a map, contour the data, and then measure the approximate distance (Δx) between selected contours representing a known head drop (ΔH). These quantities are combined to give the gradient used in eq 1. The subjectivity of measurements on a contoured map (contoured by hand or by automated methods) can be eliminated if more rigorous mathematical approaches are used. Heath (1983) presented a graphical method for solving the three-point problem in which the potentiometric surface is defined by water levels in three piezometers that form the vertices of a triangle. Pinder *et al.* (1981) and Devlin and McElwee (2007) presented purely mathematical solutions for the three-point problem. Kelly and Bogardi (1989) and Devlin (2003) presented spreadsheet methods for calculating the hydraulic gradient assuming a planar potentiometric surface with any number of wells in the network. Pinder *et al.* (1981) noted that piezometric surfaces are commonly more complex surfaces than a simple plane. They proposed that such a surface might be more usefully described by a suite of three-point estimators, defined by well triplets, each representing a plane in a subsection of the total study area. Local departures from site-wide planarity would be revealed by variations in the smaller three-point estimators. Silliman and Frost (1998) carried forward the three-point estimator idea and developed a data analysis approach in which all possible three-point estimators in the network were identified and calculated. The scatter in hydraulic gradients diminished as the size of the estimators increased, until there was convergence on a site-wide average gradient, both in magnitude and direction. They showed that this analysis could be helpful in identifying wells with unrepresentative hydraulic heads. However, for geometrical reasons, all three-point estimators in a network are not of equal value. For example, some are formed by triangles with excessively high, or low, base to height ratios that can introduce relatively high uncertainty into the associated gradient estimates. McKenna and Wahi (2006) proposed that only estimators with base to height ratios between 0.5 and 5.0 should be considered for best results, though somewhat wider ranges could be useful, depending on the tolerance of the project. The preceding work was primarily geared at representing two-dimensional (2D) groundwater flow. Abriola and Pinder (1982) extended the idea of estimators to three-dimentional flow. Biljin *et al.* (2014) used the solution method of Devlin (2013) to solve the three-point problem for the analysis of time series data. *HydroGeoEstimatorXL* is a complimentary tool that adopts

the 2-D approach of Pinder *et al.* (1981), the solution method of Devlin (2003), and the analysis method of Silliman and Frost (1998) – subject to the estimator size constraints of McKenna and Wahi (2006) – to provide hydrogeologists with a package for preliminary spatial evaluations of hydraulic head data sets and hydraulic gradients across study sites.

3. Theory

3.1 Calculation of the hydraulic gradient

Given the equation of a plane (eq 5), where *x* and *y* are map directions and z is the hydraulic head (water level), the hydraulic gradient in the *x*-direction is obtained by differentiating *z* with respect to *x*, and the gradient in the *y*-direction is obtained by differentiating *z* with respect to *y*.

$$Ax + By + Cz - D = 0 \qquad (5)$$

$$\frac{dz}{dx} = -\frac{A}{C}$$

$$\frac{dz}{dy} = -\frac{B}{C}$$

The magnitude of the overall hydraulic gradient is given by

$$grad_{magnitude} = \sqrt{\frac{A^2 + B^2}{C^2}} \qquad (6)$$

and the direction of the gradient, measured counterclockwise from the x-axis, is given by (Devlin, 2003),

$$grad_{direction} = arctan\left(\frac{B}{A}\right) \qquad (7)$$

According to Kelly and Bogardi (1989) and Devlin (2003), eq 5 can be written for each well in a network assuming they are completed at similar depths in the same aquifer, and are well connected hydraulically. If the network consists of *n* wells, then the following system of equations can be written

$$\begin{bmatrix} x_1 & y_1 & z_1 \\ \vdots & \vdots & \vdots \\ x_n & y_n & z_n \end{bmatrix} \begin{bmatrix} A \\ B \\ C \end{bmatrix} = \begin{bmatrix} D_1 \\ \vdots \\ D_n \end{bmatrix} \qquad (8)$$

or in matrix form

$$[X][A] = [D] \qquad (9)$$

where the matrix [A] contains the coefficients for the equation of the plane. The matrix [D] contains the elevation of the water table where $x = y = z = 0$. However, for the purposes of calculating the gradient and direction of flow, this elevation is not important – note the absence of D in equations 6 and 7. Therefore, a common, arbitrary, non-zero value can be used for D_1 through D_n in the [D] matrix;
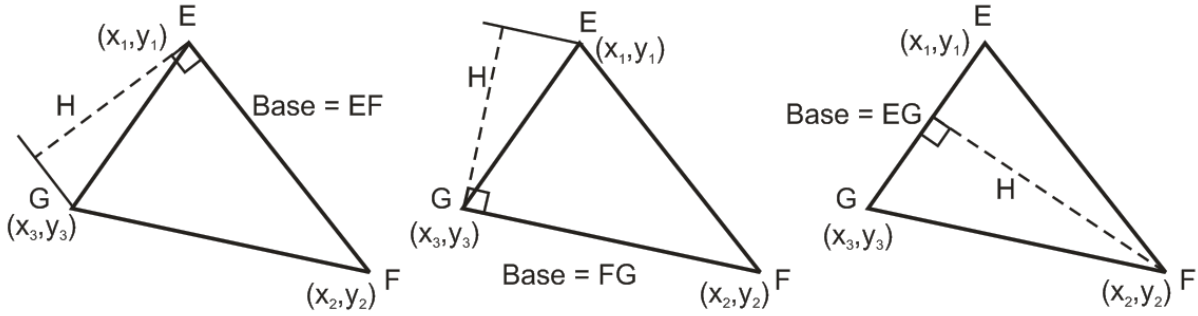
Figure 1: A hypothetical three-point estimator with vertices E, F, and G. Any of the sides can serve as the base, and the corresponding heights (H) are shown for each one. To pass the criteria of McKenna and Wahi, all three base to height ratios must be between 0.5 and 5.0.

HydrogeoEstimatorXL uses a value of 1.0. The solution to eq 9 is

$$[A] = \{[X]^T[X]\}^{-1}[X]^T[D] \qquad (10)$$

which can be solved in Excel using the methods described in detail by Devlin (2003). This equation is solved for a site-wide best fit plane to describe the piezometric surface, and for each of the three-point estimators generated in the software. The assumption of planarity may be challenged in the case of unconfined aquifers, especially where the site-wide best fit plane is concerned. However, as previously mentioned, examination of the hydraulic gradients in the local scale three-point estimators can reveal serious departures from linearity.

By default, eq 6 is evaluated by Excel to give angles between +90º and -90º from the x-axis, i.e., only vectors with a flow component in the positive x-direction are returned by Excel. If the flow direction is in the negative x-direction, an angle between +90º and -90º will be reported that is 180º from the true flow direction. *HydrogeoEstimatorXL* overcomes this limitation by determining the highest and lowest head values at selected locations on the x-axis, and on the y-axis using the equation of the plane from eq 10. From these, the general flow direction can be deduced and the flow angle automatically corrected by 180º, if necessary.

3.2 Acceptance and Rejection of Estimators

Estimators are accepted if

1) their base to height ratios are within a range specified by the user. By default, the range of 0.5 to 5.0, is entered in *HydrogeoEstimatorXL,* as recommended by McKenna and Wahi (2007);

2) either the base or the height is within a length specified by the user. This criterion permits users to screen out estimators of excessive size;

3) if the difference between maximum and minimum head values in the estimator exceeds the measurement error by a prescribed amount set by the user.

In order to calculate a base to height ratio (*Base/H*) of an estimator, the lengths of each side of the triangle are calculated from

$$EF = \sqrt{(x_1 - x_2)^2 + (y_1 - y_2)^2} \qquad (11)$$
$$EG = \sqrt{(x_1 - x_3)^2 + (y_1 - y_3)^2} \qquad (12)$$
$$FG = \sqrt{(x_2 - x_3)^2 + (y_2 - y_3)^2} \qquad (13)$$

where the terms in eqs 11 through 13 are defined in Figure 1.

The areas of the estimators are calculated using Heron's Formula (Beyer, 1973),

$$p = \frac{EF + EG + FG}{2} \qquad (14)$$

$$Area = \sqrt{p(p - EF)(p - FG)(p - EG)} \qquad (15)$$

and heights (*H*) are calculated from

$$H = \frac{2(Area)}{Base} \qquad (16)$$

The second criterion for acceptance depends on the maximum head drop across the estimator and the measurement error. If the measurement error exceeds the observed change in head across an estimator, then the hydraulic gradient within that estimator is too low to measure. This might occur, for example, in estimators formed from closely spaced wells. Estimators with no measurable gradient in them are screened out of the analysis by HydrogeoEstimatorXL. To put this into practical terms, typical water level measurements can be acquired with accuracies of about ±1 cm, though slight improvements on this can be realized with well-calibrated pressure transducers

(Devlin and McElwee, 2007). Higher uncertainties may occur depending on the skill of the operator, or the condition of the wells. If ±1 cm is representative of the measurement standard deviation, then the uncertainty envelope it defines contains the true water level with about 68% confidence. Similarly, ±2 cm would define an envelope with a 95% confidence of including the correct value, and ±3 cm would include the correct value with 99% confidence. Since the acceptance criterion is based on a difference in water levels across an estimator (Maximum – Minimum), the uncertainty must be propagated through the calculation.

$$\sigma_{\Delta WL} = \sqrt{2(\sigma_{WL})^2} \qquad (17)$$

where $\sigma_{\Delta WL}$ is the uncertainty on the difference and σ_{WL} is the uncertainty on the measurement. From this calculation, the ΔWL to achieve a confidence level of 68% is ± 1.4 cm, 95% is ±2.8 cm, and 99% is ±4.2 cm. In *HydrogeoEstimatorXL* the user can specify both the measurement uncertainty (σ_{WL}) and the confidence level desired for estimator acceptability on the Input sheet. The uncertainty on ΔWL is computed during the program execution.

3.3 Graphical Displays

HydrogeoEstimatorXL displays the results of the analysis in several ways. A map view of the study area with the locations of up to 20 wells in a network plotted to scale, and up to 24 three-point estimator triangles plotted on the site map (more estimators renders the graphic too busy to read easily), a vector map showing the location of the estimator centroids with vector tails indicating the flow direction and the distance an unretarded solute would travel in a time specified by the user, histograms of the gradient (for magnitude and direction), and groundwater speed (based on user-provided site-wide values of *K* and *n*, and eq 3), and a Silliman and Frost (1998) style estimator graphic plotting gradient magnitude, calculated from equation 6, against estimator area. With the exception of the vector map, all the graphics plot values calculated from the equations presented above.

The vector map is generated as follows. Centroids of the estimators are calculated from

$$x_{centroid} = \frac{x_1 + x_2 + x_3}{3} \qquad (18)$$

$$y_{centroid} = \frac{y_1 + y_2 + y_3}{3} \qquad (19)$$

where x_i, y_i are the map coordinates of the estimator vertices. The vector tails are plotted as straight lines of length determined by the average distance water would travel from the centroids in time, τ. The coordinates of the vector tail termini are calculated from

$$x_{endpoint} = x_{centroid} + \tau cos(\theta)\frac{K}{n} grad \qquad (20)$$

$$y_{endpoint} = y_{centroid} + \tau sin(\theta)\frac{K}{n} grad \qquad (21)$$

where θ is the angle from the x-axis to the flow direction (measured counter-clockwise), *grad* is the magnitude of the estimator gradient, *K* is the bulk hydraulic conductivity for the site and *n* is the effective porosity of the aquifer.

3.4 Mass Discharge Across a Transect

In addition to solving for the hydraulic gradient of each three-point estimator, *HydrogeoEstimatorXL* calculates the site-wide gradient using the water level data from all wells simultaneously (Devlin, 2003). For a transect cutting across the site between points (x_1, y_1) and (x_2, y_2), a parallel transect that passes through the origin of the coordinate grid can be calculated by subtracting (x_1, y_1) from both end points, leading to the vector $\vec{O}$ with endpoint (x_2-x_1, y_2-y_1).

A vector normal to this transect, $\vec{N}$ can be obtained by rearranging the dot product as follows

$$\vec{O} \cdot \vec{N} = (x_2 - x_1) \cdot x_3 + (y_2 - y_1) \cdot y_3 = 0$$
$$y_3 = \frac{(x_2 - x_1) \cdot x_3}{(y_2 - y_1)} \qquad (22)$$

where x_3 and y_3 are the coordinates of the normal vector. The value of x_3 can be arbitrarily selected in eq 22 to solve for y_3. The equation of the site-wide potentiometric surface plane (eq 5) can then be used to determine the hydraulic heads at (0,0) and (x_3, y_3), from which the hydraulic gradient perpendicular from the original transect can be calculated. The advective mass flux, *J*, and the mass discharge, M_Q, of a solute crossing the transect can be determined from

$$J = CKgrad \qquad (23)$$
$$M_Q = JA \qquad (24)$$

where *C* is the concentration of the solute crossing the transect (M/L^3), *K* is the site bulk hydraulic conductivity (L/T), and *grad* is the hydraulic gradient perpendicular to the transect, and *A* is the area of the transect. If a transect is constructed from several segments, these calculations can be performed on each segment and the corresponding equations become

$$J_i = C_iKgrad \qquad (25)$$
$$M_{Qtot} = \sum_1^m J_iA_i \qquad (20)$$

where the subscript *i* refers to each individual segment of the overall transect, and *m* is the number of segments.

4. Overview of *HydrogeoEstimatorXL*

HydrogeoEstimatorXL is an Excel workbook consisting of eight worksheets (Table 1). To begin using the software, the user enters the well location coordinates and water levels into the table in the Input sheet (Figure 2). Access to the analysis functions is gained through the dashboard. The dashboard is made available by clicking on the "Launch Dashboard" button above the input table. The dashboard offers several options including 'Clear' that resets the workbook but leaves the input table unaltered, 'Clear All' that resets the workbook and clears the input table, 'Calculate . . . ' that generates the estimators and performs all related calculations, 'Update . . .' that refreshes the histogram graphics, 'Choose Estimators' that opens a
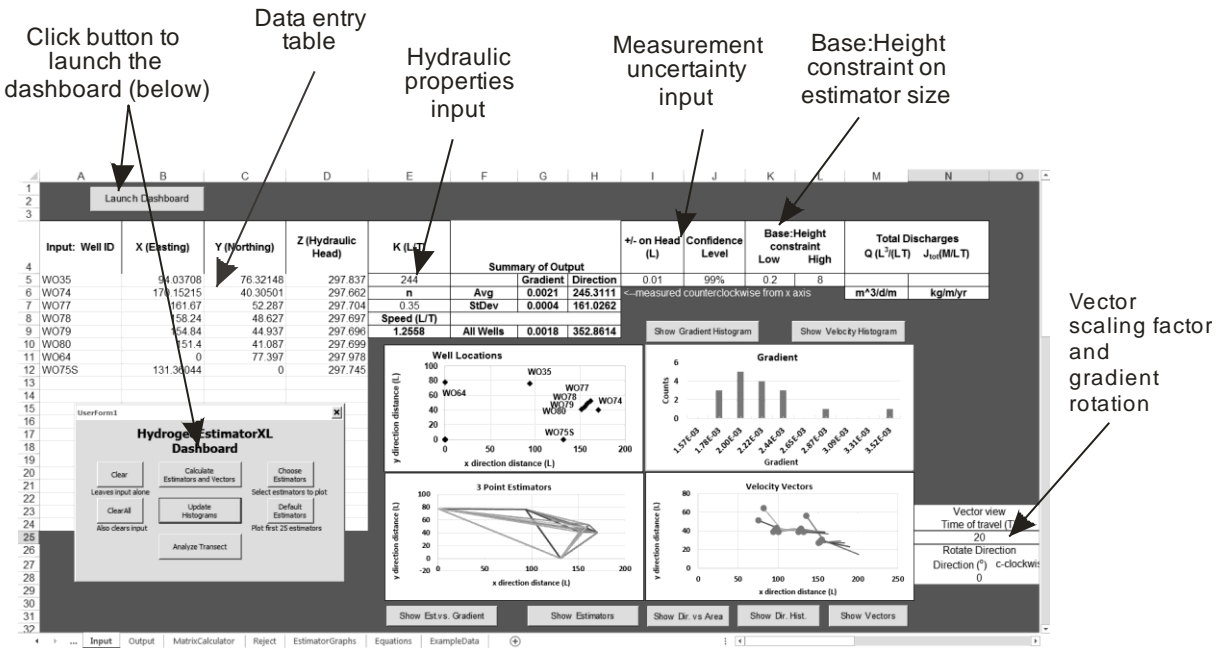
Figure 2: Annotated Input sheet in HydrogeoEstimatorXL.

dialogue box prompting the user for well triplets to plot – useful for simplifying the graphics or examining specific estimators – and 'Default Estimators' that returns the graphics to the default displays. The software was developed with Excel 2013 and the histogram plots require that users have the Analysis Tool Pak add-in active in the workbook. Without the add-in, errors involving "ATPVBAEN.XLAM!Histogram" may result. Excel 2010 suffers the same error affecting histogram generation, but operates normally with regard to the other functions. Earlier versions of Excel have not been tested. Histograms can still be generated manually in the event of the above error.

Table 1:   Summary of the worksheets found in HydrogeoEstimatorXL.

Worksheet name	Comment
Introduction	User manual that explains the use the software in detail
Input	Input sheet where the user enters the well locations, water level data, measurement uncertainty and confidence level for the calculations, and the hydraulic properties of the aquifer for groundwater velocity estimation
Output	Output repository where information concerning the accepted estimators is listed, and where the histograms and gradient-area graphs are prepared
Matrix calculator	The matrix calculator for estimating the gradients for each estimator and the network as a whole
Reject	Repository of data from the estimators that did not meet the geometric and measurement uncertainty criteria
Estimator graphs	Compilation of data for the vector map and the plot of the estimator triangles
Equations	Summary of the equations used in *HydroGeoEstimatorXL,* reproduced from the Theory section above
Example data	Datasets taken from the literature

To illustrate the use of *HydroGeoEstimatorXL*, two example data sets from the literature are examined below.

4.1 Example Case 1

To illustrate the use of *HydrogeoEstimatorXL*, the dataset recently presented by Schillig *et al.* (2016) is re-examined (Figures 2 and 3). The data were obtained from the Woodstock site in Ontario, Canada, where a glacial outwash aquifer contaminated with nitrate was tested for possible remediation by *in situ* denitrification. The input data and settings can be found in Figure 2. In this example, the base to height ratio criterion for the estimators was set to
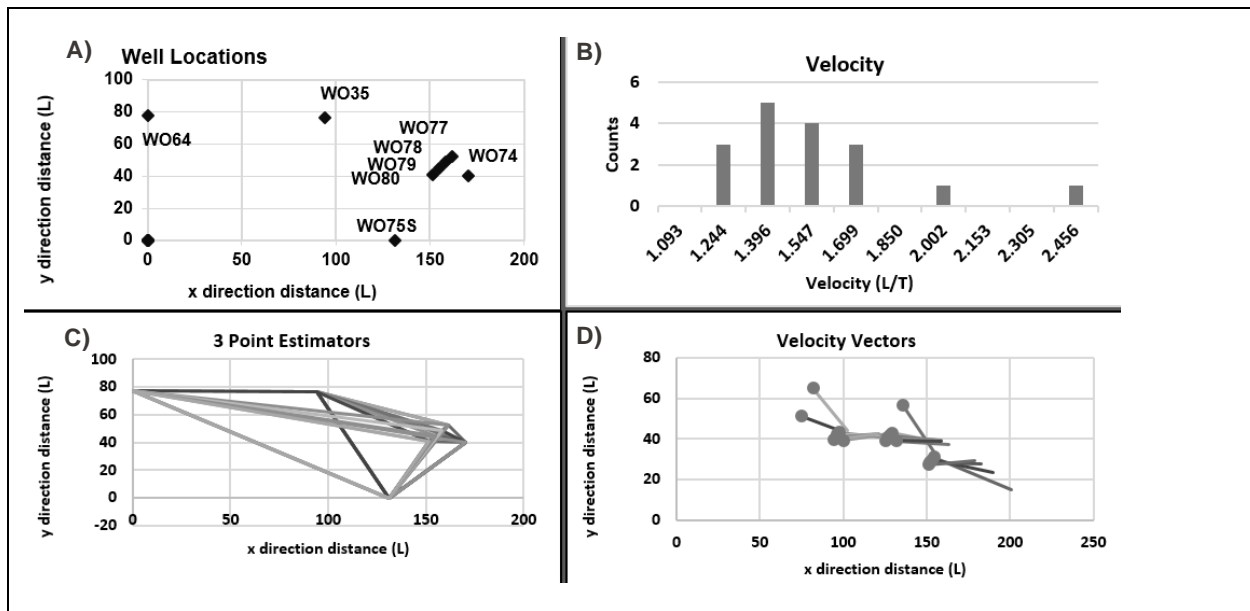
Figure 3: Screen capture of the HydrogeoEstimatorXL graphical output. (A) Site map. (B) Histogram of groundwater velocities calculated for each estimator. A site-wide value of hydraulic conductivity of 1x10^{-3} m/s and a porosity of 0.3 were assumed for these calculations. (C) Graphic showing the locations and sizes of all 17 accepted estimators. (D) Vector diagram showing estimator centroids (symbol) and vectors illustrating the flow directions associated with each estimator, and the distance traveled in one month based on the average groundwater velocity on the site.
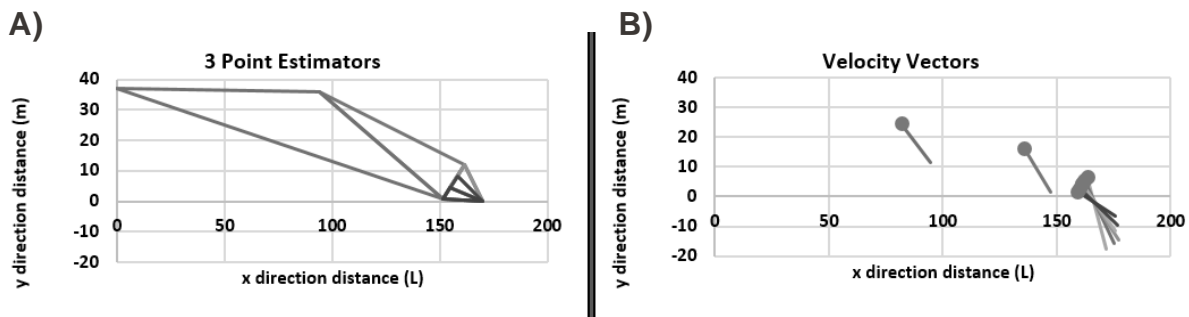

Figure 4: Screen capture of the HydrogeoEstimatorXL graphical output. (A) Site map showing locations of estimators without WO75S. (B) Revised velocity vectors (confidence interval relaxed to 66% for illustration purposes). The velocity magnitude changed little with the omission of WO75S, but the directions increased in uniformity.

0.2<B/H<8, for illustrative purposes. A site-wide hydraulic conductivity of 244 m/d and a porosity of 0.35 were assumed, based on Critchley *et al.* (2014). The analysis

performed by *HydrogeoEstimatorXL* indicated a hydraulic gradient across the site ranging from 1.5×10^{-3} to 3.5×10^{-3}, leading to estimated average groundwater velocities between 1.0 and 2.5 m/d (Figure 3B) and flow directions ranging from 45° south of east to 7° north of east (Figure 3D), with two groupings: those that indicate eastward flow and those that indicate south-eastward flow.

The estimators associated with specific vectors can be identified on the "Estimator Graphs" sheet. An examination of these associations reveals that all the estimators with predominantly eastward trending flow are associated with well WO75S, located on the south side of the site. The consistency of the vector lengths in Figure 3D indicates the water table is relatively planar; systematic changes in the vector lengths would indicate a nonplanar water table. Repeating the analysis without the WO75S well leads to a subset of estimators with a similar overall range of gradients and estimated groundwater velocities, but with two important updates to the analysis (Figure 4):
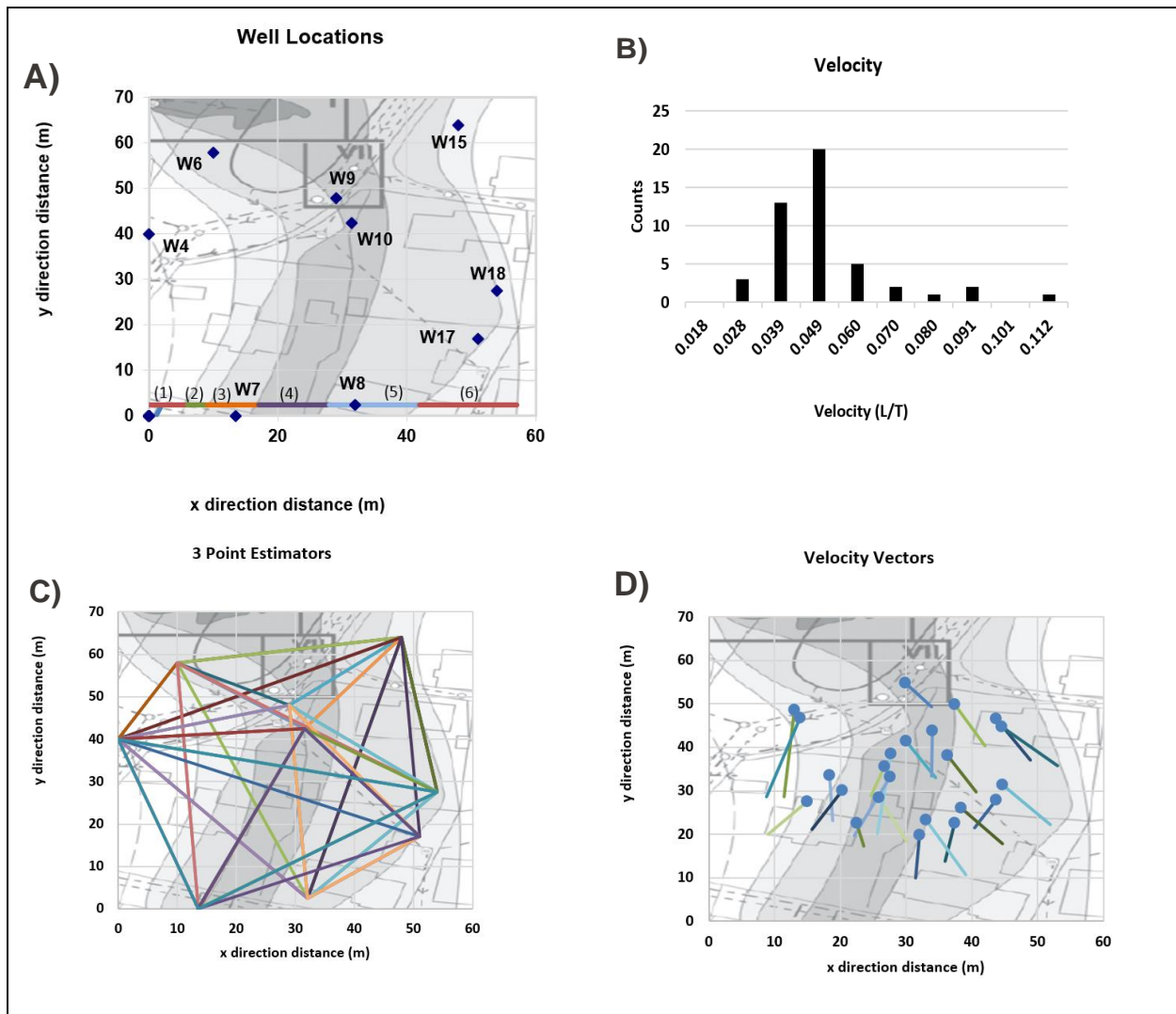
Figure 5: (A) Site map with the approximate locations of nine monitoring wells and a control transect comprising 6 segments indicated by bracketed numbers. North is in the direction of the x-axis. (B) The distribution of groundwater velocity values determined from 47 successful estimators. The velocities were calculated from the hydraulic gradients from each estimator, an assumed site-wide value of hydraulic conductivity of 10 m/d, and an effective porosity of 0.35. (C) Locations of 24 selected estimators. (D) Velocity vectors showing the locations of the 24 estimator centroids and lines depicting travel distances of water over a 60 day time period.

1) The uniformity of the flow directions improves markedly with an overall trend changing from eastward to the southeastward, in agreement with independent experimental evidence (see Schillig *et al.*, 2016). This result strongly suggests that WO75S was in poor hydraulic connection with the remainder of the network and that it biased the analysis.

2) The number of estimators in the analysis decreased by half, from 17 to 8. This occurred because the location of WO75S made it possible estimators with WO75S increased the weighting of that well on the overall assessment of flow at

the site. Therefore identification of the well as problematic, and its removal from the analysis was to construct numerous estimators with favorable base to height ratios.

3) The number of estimators in the analysis decreased by half, from 17 to 8. This occurred because the location of WO75S made it possible to construct numerous estimators with favorable base to height ratios. The large number of estimators with WO75S increased the weighting of that well on the overall assessment of flow at the site. Therefore identification of the well as

problematic, and its removal from the analysis was very important for improved accuracy of the analysis, particularly where flow direction was concerned.

A well may be associated with an anomalous water level (compared to the other wells in a network) for several reasons, including: 1) poor hydraulic connection due to geological reasons – for example a well might be completed in geologic stratum with a weak or absent hydraulic connection to the sediment(s) hosting the remainder of the network. This could occur in association with heterogeneous sediments and be exacerbated by large horizontal or vertical separation distances between wells; 2) lack of hydraulic equilibrium – for example poor well screen development or low permeability media around the well could prevent timely water level equilibration; foreign objects in a piezometer could isolate the standing water column from the screen, delaying the development of equilibrium water levels; 3) transience in the flow system - outside influences, such as pumping, might affect one well in a network disproportionately during a coincident water level collection effort; 4) operator or data handling errors – for example, an error could be made reading the depth to water with a sonde and tape, or a transducer might fall out of calibration; errors could occur in the surveying of a well, resulting in an inaccurate elevation assigned to the top of casing and subsequently to calculated water level elevations.

HydrogeoEstimatorXL provides a means of identifying a well or wells that might suffer from one or more of the problems above, but does not identify the specific cause. Users must decide from other information, or professional judgement, whether or not discarding data from a particular well is justified. The results of the analysis of the Woodstock data above are in agreement with the findings reported by Schillig *et al.* (2016), who used independent, custom software (also executed in Excel) to come to the same conclusion. This analysis augmented the previous one with graphical displays of ranges of velocity, gradient, flow direction, mapped renditions of the estimators themselves, and the velocity vectors associated with them. The additional graphics provide a rapid means of acquiring an intuitive understanding of a flow system. As illustrated above, this can be very useful in identifying issues requiring further scrutiny.

4.2 Example Case 2

A metal-processing plant in central Denmark was found to have discharged tetrachloroethene (PCE) into a sewer line that was subsequently discovered to be leaky (Fjordboge *et al.*, 2012). Some of the PCE entered the underlying water table aquifer comprising layered sands, silts and clays. A plume developed that carried PCE and anaerobic degradation products, including 1,2 dichlorothene (12DCE) eastward through the town of Skuldelev. Since the year 2000, over 200 monitoring wells were installed in and around the source area to delineate the contaminated area and gain insight into the hydrogeology of the site. A control transect consisting of multilevel wells was established across the plume on the east side of source area, with the aim of

determining the advective mass flux of contaminants leaving the site. Using water level data reported by Lange *et al.* (2011), and concentrations of c12DCE reported by Troldborg *et al. (*2012), *HydrogeoEstimatorXL* was used to estimate the flux of c12DCE across the control transect (Figure 5 A).

Troldborg *et al.* (2012) examined the distribution of c12DCE with multilevel monitors along the transect, and more than 100 water analyses, and found that indeed most of the contaminant did cross the transect within about a 38 m^2 zone between 0 and 3.5 meters above sea level. The various methods used to estimate the contaminant discharge across the transect yielded values ranging from 4.3 – 1.8 kg/yr to 7.1 – 6.3 kg/yr.

HydrogeoEstimatorXL calculated that the majority of the mass crossing the transect does so at segment (4), which was assumed to be 11 m long with an effective concentration of 30 mg/L based on the plume figure presented by Troldborg *et al*. (2012, Figure 7, pg. 12) (Figure 5A). The total mass discharge across the transect was estimated to be on the order of 2.1 kg/yr per meter of depth. If the depth range of importance, based on the multilevel data and Figure 3 in Troldborg *et al.* (2012), was about 3.5 m, the *HydrogeoEstimatorXL* estimate becomes 7.4 kg/yr. This estimate is comparable with the range reported by Troldborg *et al.* (2012), discussed above. The relatively simple assumptions built into the *HydrogeoEstimatorXL* calculations means that they should not be substituted for field data. Nonetheless, the fact that preliminary estimations of mass discharge suitable for problem identification is demonstrated by the favorable results.

5. Conclusions

HydrogeoEstimatorXL is a convenient tool freely available to professionals to assist with the interpretation of water level data. The graphical output, in the form of velocity vector maps and histograms of the hydraulic gradient, flow direction, and approximate groundwater velocity, can be instrumental in gaining an intuitive understanding of the groundwater flow through an area, and in identifying wells that might not be well connected with the monitoring or piezometric network. *HydrogeoEstimatorXL* also permits users to define a transect, with unit depth, across the study area, and then estimate the mass discharge of dissolved substances across the transect plane. Data of these kind are likely to be useful in the early stages of site investigations and with problem definition. They may also be useful in reviews and quality control checks on flow and transport characteristics, calculated independently by other means.

References

Abriola, L.M., Pinder, G.F. (1982) Calculation of velocity in three space dimensions from hydraulic head measurements. Ground Water, 20(2): 205-213

Beyer, W.H. (1973) CRC Standard Mathematical Tables, 25th Edition. CRC Press, Boca Raton, USA

Biljin, M., Ross, R.R., Acree, S.D. (2014) 3PE: a tool for estimating groundwater flow vectors. EPA, Office of Research and Development National Risk Management Research Laboratory, Ground Water and Ecosystems Restoration Division, EPA 600/R-14/273, September 2014, www.epa.gov/ada

Butler, J. J. (1997). The Design, Performance, and Analysis of Slug Tests. CRC Press,Technology & Engineering, Boca Rotan, USA

Butler, J.J., Dietrich, P., Wittig, V., Christy, T. (2007). Characterizing hydraulic conductivity with the direct-push permeameter. Ground Water, 45(4): 409-419

Butler, J.J.jr., Healey, J.M., McCall, G.W., Garnett, E.J., Loheide, S.P. (2002) Hydraulic tests with direct-push equipment. Ground Water, 40(1): 25-36

Critchley, K., Rudolph, D., Devlin, J.F., Schillig, P.C. (2014) Stimulating in situ denitrification in an aerobic, highly permeable municipal drinking water aquifer. Journal of Contaminant Hydrology, 171: 66-80.

Devlin, J.F. (2003) A spreadsheet method of estimating best-fit hydraulic gradients using head data from multiple wells. Ground Water, 41(3): 316-320

Devlin, J.F., McElwee, C.D. (2007) Effects of measurement error on horizontal hydraulic gradient estimates. Ground Water, 45(1): 62-73

Fjordboge, A.S., Lange, I.V., Bjerg, P.L., Binning, P.J., Riis, C., Kjeldsen, P. (2012) ZVI-Clay remediation of a chlorinated solvent source zone, Skuldelev, Denmark: 2. Groundwater contaminant mass discharge reduction. Journal of Contaminant Hydrology, 140-141: 67–79.

Freeze, R.A., Cherry, J.A. (1979) Groundwater. Prentice Hall, New Jersey, USA

Heath, R.C. (1983) Basic Ground-Water Hydrology. U.S. Geological Survey Water-Supply Paper 2220.

Kelly, W.E., Bogardi, I. (1989) Flow directions with a spreadsheet. Ground Water, 27(2): 245-247

Knight, R. (2001) Ground penetrating radar for environmental applications. Annual Review of Earth and Planetary Sciences, 29: 229-255

Kruseman, G.P., de Ridder, N.A. (1991) Analysis and evaluation of pumping test data, 2nd edition. International Institute for Land Reclamation and Improvement, Publication 47, Wageningen, The Netherlands

Lange, I.V., Troldborg, M., Santos, M.C., Binning, P.J., and Bjerg, P.L. (2011) Kvantificering af forureningsflux i transekt ved Skuldelev. Datarapport et samargjdsprojekt mellem, DTU Miljø og Region Hovedstaden (Quantification of contaminant flux in transects at Skuldelev. Data Report of a joint project between DTU Environment and the Capital Region), Denmark

Legchenko, A., Baltassat, J.M., Beauce, A., Bernard, J. (2002) Nuclear magnetic resonance as a geophysical tool for hydrogeologists. Journal of Applied Geophysics, 50: 21– 46

McKenna, S.A., Wahi, A. (2006) Local hydraulic gradient estimator analysis of long-term monitoring networks. Ground Water 44(5): 723-731

Molz, F.J., Morin, R.H., Hess, A.E., Melville, J.G., Guven, O. (1989) The impeller meter for measuring aquifer permeability variations: evaluation and comparison with other tests. Water Resources Research, 25(7): 1677-1683

Pinder, G.F., Celia, M., Gray, W.G. (1981) Velocity calculation from randomly located hydraulic heads. Ground Water, 19(3): 262-264

Schillig, P.C., Devlin, J.F., Rudolph, D. (2016) Upscaling point velocity measurements to characterize a glacial outwash Aquifer. Groundwater, 54(3): 394-405

Silliman, S.E., Frost, C. (1998) Monitoring hydraulic gradient using three-point estimator. Journal of Environmental Engineering, 124(6): 517-523

Troldborg, M., Nowak, W., Lange, I.V., Santos, M.C., Binning, P.J., Bjerg, P.L. (2012) Application of Bayesian geostatistics for evaluation of mass discharge uncertainty at contaminated sites. Water Resources Research, 48, W09535, doi:10.1029/2011WR011785.

Zemansky, G., Devlin, J.F. (2013) Point velocity probe technology transfer. GNS Science Consultancy Report 2013/199, August, New Zealand